

## Stratal disruption and development of mélangé, Western Newfoundland: effect of high fluid pressure in an accretionary terrain during ophiolite emplacement

J. W. F. WALDRON, D. TURNER\* and K. M. STEVENS†

Geology Department, Saint Mary's University, Halifax, Nova Scotia, Canada B3H 3C3

(Received 31 August 1987; accepted in revised form 10 July 1988)

**Abstract**—The Bay of Islands Ophiolite was emplaced onto the continental margin of North America during the mid-Ordovician Taconic orogeny, when tectonic slices of continental margin sediments were accreted to the moving allochthon. Tectonic slices grade into and are surrounded by mélangé. Early fracture in sandstones formed without grain breakage and allowed penetration of liquid petroleum along fracture planes. Other fractures involved cataclastic flow and were sometimes re-activated during formation of later pressure solution cleavage. Shear-fracture and extension-fracture boudinage affect competent strata; extensional veins cut cement in limestone beds and are filled by shale, quartz, calcite and bitumen. Folds also formed, at a time when siltstone and sandstone were at least partially lithified. Mélangé matrix shows abundant shear and extension fractures in a variety of orientations.

Coaxial extension responsible for disruption of bedding can be explained by a brittle accretionary wedge model in which high fluid pressures resulted from tectonic dewatering of shales. Surface slope decreased as fluid pressure rose beneath the ophiolite, causing horizontal extension of the wedge. After escape of excess water the surface slope steepened again as renewed stacking occurred.

### INTRODUCTION

THE Bay of Islands Ophiolite was emplaced onto the eastern margin of the North American continent during the Middle Ordovician Taconic orogeny, interpreted by Malpas & Stevens (1977) as a collision of the continent with an E-dipping subduction zone. During the emplacement of the ophiolite, continental margin sediments were deformed and accreted to the base of the moving allochthon as a series of tectonic slices (the Humber Arm Slice Assemblage) surrounded by disrupted, apparently chaotic zones termed mélanges (Stevens 1965, 1970). The tectonic setting of this assemblage is similar to that of foreland fold and thrust belts elsewhere along the northwest ('external') margin of the Appalachian system and other mountain belts. It differs strikingly from these belts in the disorganized configuration of its tectonic slices, which do not always show older-over-younger relationships at thrust contacts, and in the abundance of disrupted stratification and mélangé. This paper aims to document the small-scale structures produced in the Humber Arm Slice Assemblage by the emplacement event. We show that high fluid pressures, due to both water and liquid hydrocarbons, existed within the deforming allochthon and compare the features of the slice assemblage with a theoretical model for accretionary wedges undergoing failure by brittle fracture, in order to show that high fluid pressures can account for coaxial bed-parallel extension within the sediments of the Slice Assemblage.

Figure 1 summarizes the general geology and stratigraphy of the Bay of Islands area. Three major tectonic units are present. Lowest in the structural pile are massive platform carbonates representing the apparently autochthonous Cambro-Ordovician continental shelf of North America. Outside the area of Fig. 1 these rest unconformably on basement gneisses of Grenvillian age.

The tectonically overlying Humber Arm Slice Assemblage also consists of Cambro-Ordovician sediments, but these show predominantly turbiditic (and occasionally pelagic) facies indicative of continental slope and rise environments (James & Stevens 1982). The stratigraphy was deduced by Stevens (1965) from partial sequences in numerous tectonic thrust slices. Paleocurrents indicate transport from a continental shelf that lay to the present-day west. At the top of the stratigraphic succession are early Ordovician coarse turbiditic sandstones ('easterly derived flysch'), believed to have been derived from the advancing allochthon. The tectonic slices are separated by zones in which sandstones and limestones occur as blocks immersed in a shaly matrix. These mélangé zones show gradational contacts with the deformed marginal parts of slices. 'Exotic' lithologies are rare to non-existent: even occasional blocks of mafic volcanic and hypabyssal rocks have possible correlatives at the base of the stratigraphic sequence in the highest tectonic slice. Mélangé is therefore defined on the basis of its lack of a coherent stratigraphy; the distinction between the smallest tectonic slices and the largest blocks in the surrounding mélangé is mainly one of scale.

Overlying the Humber Arm Slice Assemblage is the Bay of Islands Complex, which displays a complete ophiolite sequence with peridotites of inferred mantle

\* Present address: Noranda Exploration, P.O. Box 66, Ming's Bight, Newfoundland, Canada A0K 3S0.

† Present address: Applied Geoscience B., Whiteshell Nuclear Research, Pinawa, Manitoba, Canada R6E 1L0.

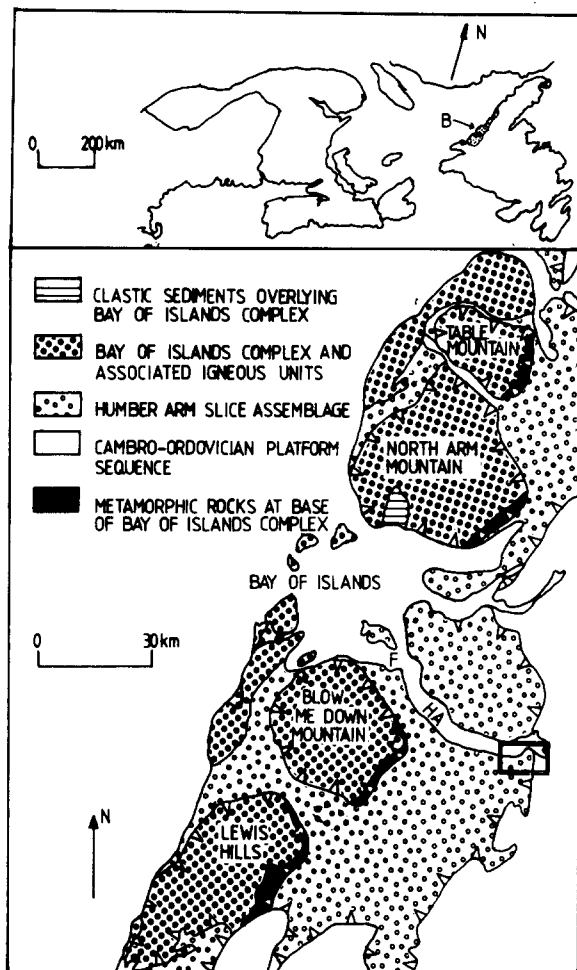


Fig. 1. Top: Map showing location of Bay of Islands in western Newfoundland. B = Bay of Islands. Stipple: Ordovician allochthons. Bottom: Schematic map showing major tectonic units in Bay of Islands area. Box encloses area of Fig. 2. Localities mentioned in text: F = Frenchman's Cove; HA = Humber Arm.

origin at the base. The Complex consists of four separate klippen. Between the peridotites of North Arm Mountain and the uppermost deformed sediments of the Humber Arm Slice Assemblage is a thin (*ca* 150 m) layer of metamorphic rocks well exposed on the north shore of the Bay of Islands (Fig. 1), showing an inverted metamorphic zonation from amphibolite-facies close to the peridotites to greenschists farther away. McCaig (1983) has deduced pressures of 7–11 kbar and temperatures of 750–850°C in these metamorphic rocks. The metamorphic rocks are believed to record progressive uplift of the ophiolite as it was emplaced. The lowest metamorphic rocks are phyllites which are lithologically similar to the most highly deformed rocks of the Humber Arm Slice Assemblage below.

#### STRUCTURE OF THE HUMBER ARM SLICE ASSEMBLAGE

Megascopic and mesoscopic structural features of the slice assemblage have been described by Stevens (1965) and Waldron (1985). Within the assemblage, soft sediment deformation features such as pseudonodules, ball-

and-pillow structure and slump folds occur sporadically in turbiditic sandstone sequences. Sandstone dykes are well displayed at the base of the easterly derived flysch on the north coast of Humber Arm; a complex of sandstone dykes and sills surrounding coherent sandstone and shale blocks occurs within the flysch at Middle Arm Point (Stevens 1965). Individual tectonic slices show a coherent stratigraphic sequence and are generally right-way-up, although localized overturning of strata occurs on the limbs of recumbent, W-facing ( $F_1$ ) folds; in contrast to slump folds, these deform the bed-parallel fissility fabric of the shales. The slices do not show the consistent older-over-younger relationships at tectonic contacts that characterize some foreland thrust belts (e.g. Dahlstrom 1970, Boyer & Elliott 1982), suggesting that either out-of-sequence thrusts or low-angle normal faults may be present. Towards the edges of slices, beds are increasingly deformed by shear-fracture and extension-fracture boudinage and by W-facing asymmetric folds. The slices are surrounded by more disrupted domains termed *mélange*, in which beds of competent lithologies (sandstone, limestone) have been reduced to lozenge-shaped or ovoid blocks surrounded by a generally friable shale matrix with a tectonic fabric. Some blocks have smooth bulbous surfaces resembling load structures, but others have the rubbly surface texture shown in Fig. 3(a).

The entire allochthon is affected by upright ( $F_2$ ) folds trending roughly N–S which overprint emplacement-related structures (Waldron 1985). Mapping in the Corner Brook area (Fig. 2) shows that the thrust slices, intervening *mélange* zones and underlying platform carbonates are folded, confirming this interpretation. On the east slope of Crow Hill (Fig. 2) the *mélange* contains a large (20 m) block of mafic volcanic rock; elsewhere only disrupted Humber Arm lithologies are present. The folds and associated axial plane cleavage ( $S_2$ ) increase in intensity eastwards across the allochthon. According to Casey & Kidd (1981) the basal thrust of the ophiolite is folded beneath North Arm Mountain, accounting for a high Bouguer gravity anomaly there; no equivalent anomaly is seen over Blow-Me-Down Mountain, which is inferred to have a roughly horizontal basal surface.  $F_2$  folds and cleavage can be traced southwards to the Stephenville area (Williams 1985) where they affect Silurian and Devonian rocks unconformably overlying the allochthon. Some later, more localized deformation has also affected the area. Beneath Crow Hill (Fig. 2) both the early thrusts and the  $S_2$  cleavage show relatively gentle dips, probably as a result of a later open fold. Waldron (1985) described late ( $F_3$ ) folds trending generally E–W, associated with a sporadically developed axial plane crenulation cleavage. These folds produce culminations and depressions of the  $F_2$  fold axes. Bosworth (1985) has described late, E-vergent brittle thrust faults from several outcrops in the allochthon. Williams & Cawood (1986) have mapped analogous N-striking faults cutting carbonates to the south of Corner Brook, but these do not appear to affect the gross distribution of rock units in the area of Fig. 2. We interpret them as

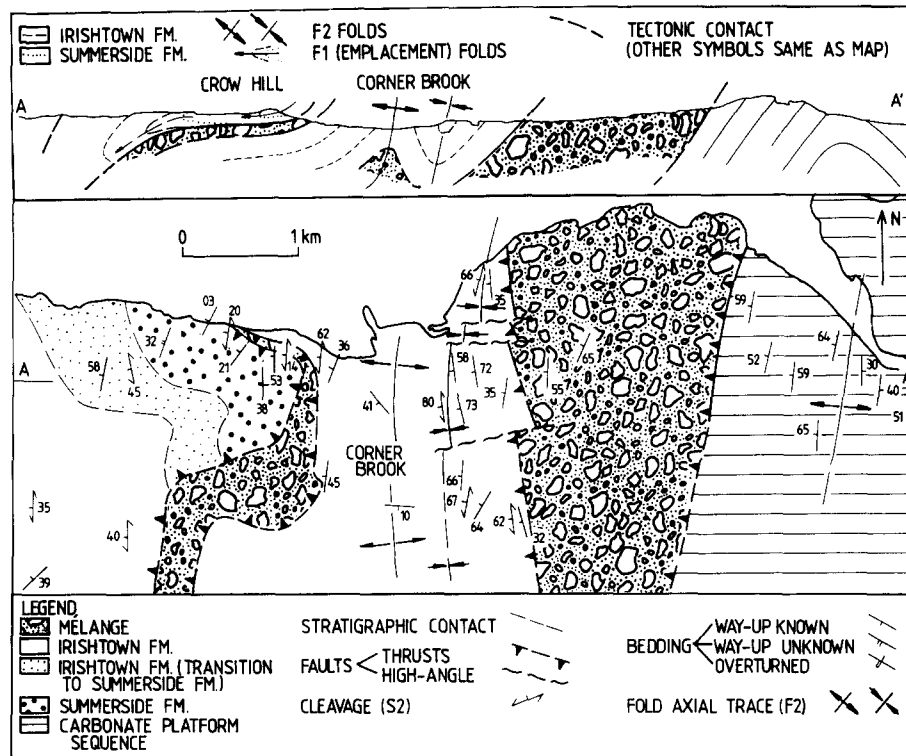


Fig. 2. Geological map and cross-section of Corner Brook (location shown in Fig. 1) showing distribution of tectonic slices and mélangé above apparently autochthonous platform sequence. Summerside Formation consists of late Precambrian or early Cambrian rift-related clastics. Irish Town Formation is overlying continental slope turbidites.

having relatively small offsets compared to the earlier W-vergent thrusts.

#### MICROSTRUCTURES AND THE DEVELOPMENT OF MÉLANGE FABRIC

The origin of fabric in many mélangé terrains is controversial: matrix fabric may be interpreted as a product of a tectonic mélangé-forming process or simply as a result of later deformation superimposed on a syndimentary olistostrome. Over-printing relationships in the Bay of Islands help to resolve this problem. A strong bed-parallel fissility is present in the coherent sediments of the tectonic slices, which developed after slump folding and other obvious soft-sediment features, but before the majority of emplacement-related deformation in and adjacent to mélangé zones. Post-emplacement structures may similarly be distinguished where  $S_2$  cleavage is developed, cross-cutting emplacement-related structures.

Transitional zones between coherently bedded sediment and mélangé are characterized by increasing deformation and disruption of bedding. Several mesoscopic features are particularly characteristic of competent beds (sandstone, limestone) in such zones, but also occur in blocks within thoroughly disrupted mélangé terrains; the features are: networks of small fractures that offset bed surfaces to produce a rubbly surface texture (Fig. 3a); extension-fracture and shear-fracture boudins (Fig. 4); and folds (Fig. 5), which typically occur in coherent terrains as asymmetric, W-vergent pairs. In

incompetent shales, scaly fabric (Fig. 6), characterized by anastomosing, sometimes polished parting surfaces, is progressively developed as bedding is disrupted.

#### Fractures

Figure 3(a) shows the 'rubbly' surface texture characteristic of some blocks of sandstone extracted from mélangé. The sandstones are probably fragments of the 'easterly derived flysch' deposited shortly before the onset of deformation. The irregularities in the surfaces of such blocks are filled with friable mélangé matrix shale which is easily removed by weathering on exposed surfaces. The block is cut by numerous fracture surfaces that appear to be of two types. Most numerous are dark, somewhat diffuse lines marked in thin section (Fig. 3b) by concentrations of bituminous organic matter that occurs interstitially to sand grains and also in cavities within diagenetically dissolved 'skeletal' alkali feldspar grains. Similar bituminous material occurs elsewhere in the sandstone in diffuse patches unrelated to fractures. Patches of calcite cement occur between sand grains along or adjacent to some of the fractures. In most cases there is no visible grain size reduction or development of preferred orientation, suggesting that movement occurred without fracturing or permanent distortion of grains. A second group of fractures, including those principally responsible for the rubbly surfaces of the blocks, are marked by concentrations of poorly sorted material, including fine-grained quartz, sericite and opaques. Similar fractures occur in older sandstones ('western sandstones' of Waldron 1985), near the con-

tacts with *mélange*. In block interiors, fractures are marked by zones of small angular quartz grains without preferred orientation, that suggest cataclastic grain size reduction (Fig. 3c). However, close to the edges of blocks, the fine-grained particulate material becomes more sericite rich; some of this material may represent particles of finer-grained sediment introduced by fluids that penetrated blocks along the fractures. Other such zones appear to have been re-activated during formation of the pressure-solution cleavage, as shown in Fig. 3(d). The pressure-solution cleavage curves from a nearly perpendicular orientation distant from the microshear, to sub-parallel at the shear itself. In contrast to Fig. 3(c), grain size reduction is accompanied by development of a preferred orientation; under crossed polars, undulose extinction and sub-grains are seen in quartz crystals within the zone. Thus the sandstones show evidence for three processes of deformation: cataclastic flow occurred first, but was overprinted by deformation due to both crystal plasticity and diffusional mass-transfer processes.

#### *Extension-fracture boudins*

Extension-fracture boudinage is common in slice margins and blocks within *mélange* and frequently produces a chocolate-tablet structure (Fig. 4a). Typical examples of such fractures are shown in thin section in Figs. 4(b) & (c). Figure 4(b) shows an extension fracture in a limestone bed, whose stepped outline indicates that it opened as a result of sliding on lamination surfaces. The fracture was initially incompletely filled and the voids were lined by 'dog-tooth' sparry calcite crystals (white in Fig. 4b). The central parts of the voids were then filled by organic material now represented by brittle opaque black pyrobitumen. Further extension (or shrinkage of the organic material) caused fracturing of both pyrobitumen and the shale fill, and was accompanied by syn-deformational growth of quartz and calcite fibres. In Fig. 4(c) a V-shaped cleft in the bed surface cross-cuts earlier calcite-filled veins, showing that the limestone was lithified at the time of boudinage. The cleft is filled by impure limestone and shale from the adjoining bed and contains fragments of the sparry calcite vein-filling cement. The normally bed-parallel fabric of the shale is tightly folded into the base of the cleft.

#### *Shear-fracture boudins*

Shear-fracture boudinage was identified in earlier papers (Bosworth 1984, Waldron 1985) as a major process of bed disruption (Fig. 4d) leading to formation of *mélange*. Movement usually occurs along discrete conjugate fractures which offset bedding in a normal sense. Fractures are typically curved, cutting competent strata (sandstone, limestone) at steeper angles and becoming asymptotic to bed-parallel fissility in the shales. Movement along such fractures produced significant rotation of bedding (Fig. 9) and eventually detached lozenge-shaped blocks. Under high magnification the shear fractures appear to be single discrete surfaces, or are marked

only by a very thin (1  $\mu\text{m}$ ) seam of 'matrix' sericite or chlorite with a preferred orientation parallel to the shear surface. The sand and silt grains are neither distorted nor obviously fractured. Very similar fracture surfaces are described from Franciscan *mélanges* by Cowan (1982), who attributed their formation to grain-boundary sliding.

#### *Folds*

Folds are widespread both in coherent terrains and in *mélange*: folds in *mélange* typically occur as isolated hinges surrounded by shale matrix. Figure 5(a) shows a recumbent fold in siltstones and shales transitional to *mélange* west of Humber Arm. The strongest and most penetrative fabric developed in the shales is fissility parallel to bedding, which can be traced round the coherently bedded part of the fold hinge in both hand sample and thin section. In the hinge region, the fissility is deformed in the finest grained material by a crenulation cleavage ( $S_1$ ) axial planar to the fold. Bedding is offset by several small faults in the fold core and on the limb, where both shear-fracture and extension-fracture boudins occur. These faults neither cut across the fold axial surface nor are they refolded; they are most reasonably interpreted as structures produced during folding. Towards the outside of the fold, bedding is highly disrupted by small anastomosing faults which contribute to an axial planar fabric seen in hand sample. This fabric resembles the scaly fabric of the *mélange* matrix. Individual beds in the disrupted part of the sample are thinned dramatically but do not show internal deformation of quartz grains; deformation was accommodated by grain-boundary sliding and shearing of the matrix between the silt grains. The fold is cross-cut by extensional fractures whose trace is perpendicular to the axial surface. Other 'radial' veins are more localized within the outer parts of siltstone layers on the fold hinge and have irregular, ragged outlines similar to the vein in Fig. 4(b), indicating that bedding-plane slip occurred as they opened. These fractures are filled with quartz and calcite in equant, essentially undeformed crystals. The distribution of fractures and boudins indicates that siltstone was more competent than shale at the time of deformation. This is confirmed by the near-parallel (class 1B) geometry of the siltstone layers, and by the distortion of the shale fabric at the corners and edges of some boudins (Fig. 5c). Thus although the folds are locally disharmonic and chaotic in style, they were produced in significantly lithified sediments. The fold is apparently cross-cut by a second crenulation cleavage; although this does not obviously deform the quartz-calcite veins, some cleavage planes can be traced into dark stylolytic surfaces that are most intensely developed where they cut or pass around the terminations of the veins. This cleavage is probably the regional  $S_2$  cleavage that post-dates thrusting.

In some areas the axial surfaces of emplacement-related folds are close to the orientation of  $S_2$  cleavage.

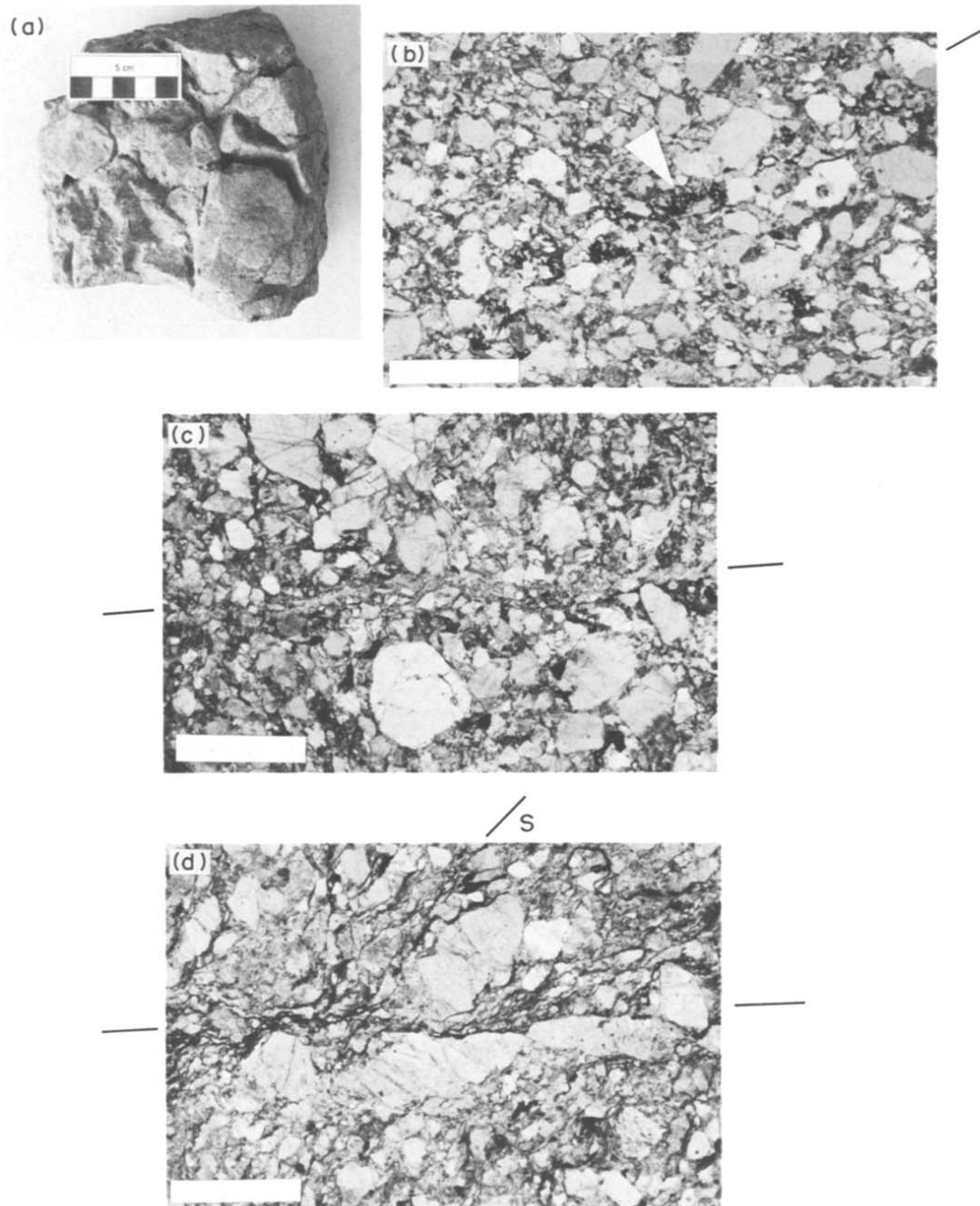


Fig. 3. Fractures in sandstones. (a) Block with rubbly surface extracted from *mélange*. Dark lines visible on surface at lower right are marked by interstitial organic matter. (b) Thin section of sample shown in (a). Fracture runs from lower left to upper right, marked by irregular line of interstitial opaque organic matter. Grain at centre (arrow) is partially dissolved 'skeletal' grain of feldspar filled with organic matter. (c) Thin section of older sandstone ('western sandstone' of Waldron 1985) showing trace of cataclastic fault running horizontally across field. (d) Shear zone in same samples as (c), interpreted as a cataclastic fracture re-activated during development of pressure-solution cleavage (marked 's'). Plane polarized light, scale bar 1 mm, in all photomicrographs.

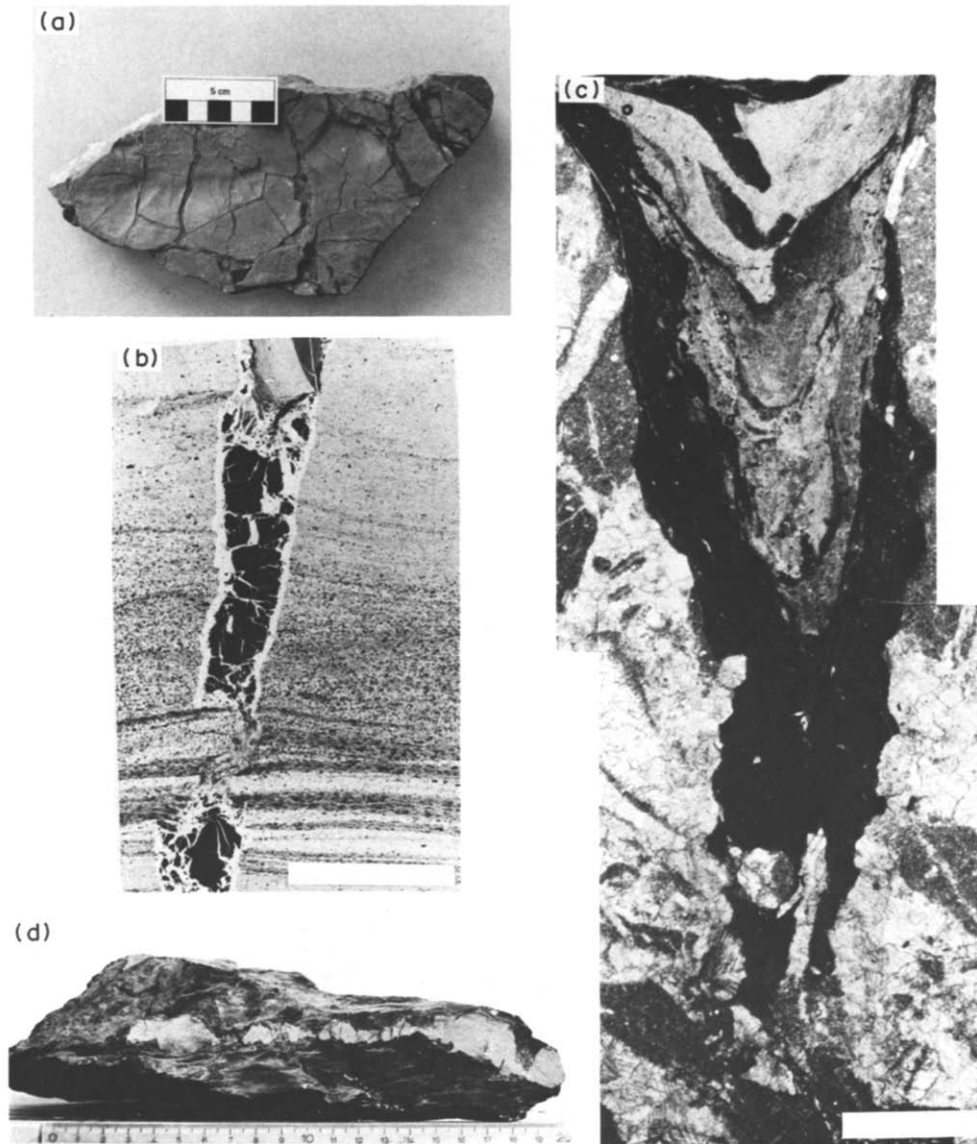


Fig. 4. (a) Extension-fracture boudinage: hand sample of bed of turbiditic limestone showing 'chocolate tablet' boudinage. (b) Thin section of similar sample. Extension fracture is filled by fragments of adjoining mudstone bed, sparry calcite and quartz (white), and pyrobitumen (black). History of fracture is discussed in text. Scale bar 1 cm. Plane polarized light. (c) Thin section of similar fracture. Fracture fill truncates vein-filling sparry calcite (light) in limestone (grey). Fracture is filled by dark grey impure limestone and paler shale from adjoining beds, deformed to fill fracture. Scale bar 1 mm. Plane polarized light. (d) Hand sample showing attenuation of dolomitic siltstone bed (pale) mainly by shear fracture boudinage. Scale bar 1 cm.

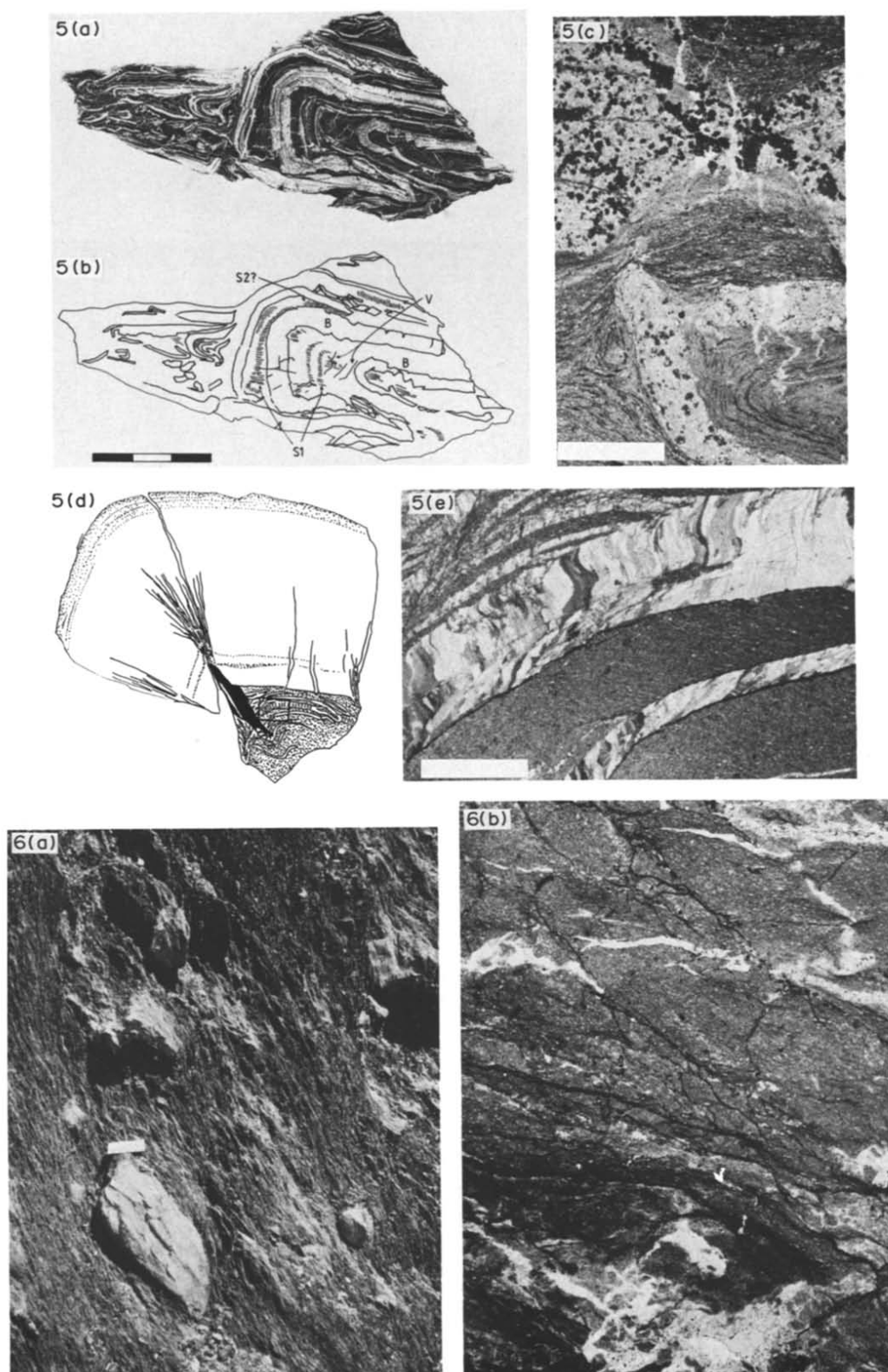


Fig. 5. Folds. (a) Isoclinal fold in siltstones and shales gradational to mélangé. Xerographic print of large format thin-section. (b) Diagram of sample (a) showing selected locations of axial plane crenulation cleavage ( $S_1$ ), later crenulation cleavage ( $S_2$ ), veins (V) and boudinage (B). Scale in cm. (c) Enlarged view of core of same fold (immediately below B in 6a) showing folding of primary shale fabric and competent behaviour of siltstone boudins. Plane polarized light. Scale bar 1 mm. (d) Drawing of fold in limestone that underwent tightening during post-emplacement folding. Stipple: impure limestone. Black: impure stylolytic limestone. Irregular pattern of lines: veins of fibrous calcite. Box: area shown in (e). (e) Fibre-filled veins from sample in (d). Crossed polars. Scale bar 1 mm.

Fig. 6. Mélangé. (a) Field appearance of mélangé. Scale bar 10 cm. (b) Thin section of mélangé matrix under plane polarized light, showing shear fractures (dark), some of which may be modified by later pressure solution in lower part of diagram. Quartz veins appear white and are apparently undeformed. Note complex mass of vein quartz (undeformed) low in photograph. Scale bar 1 mm.

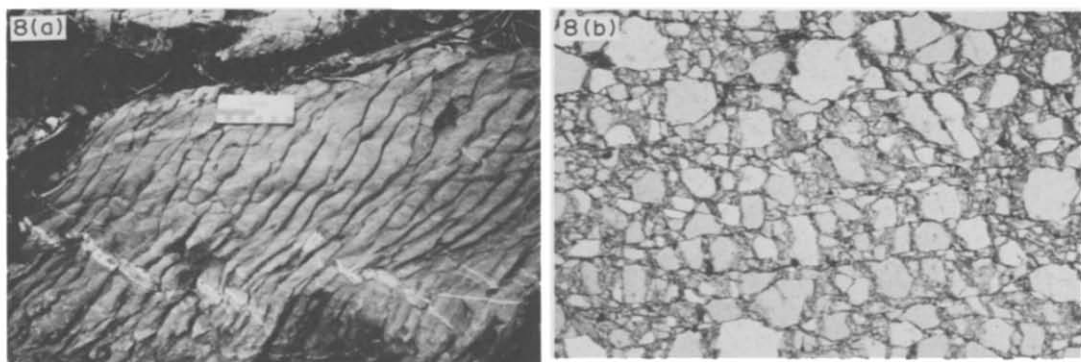
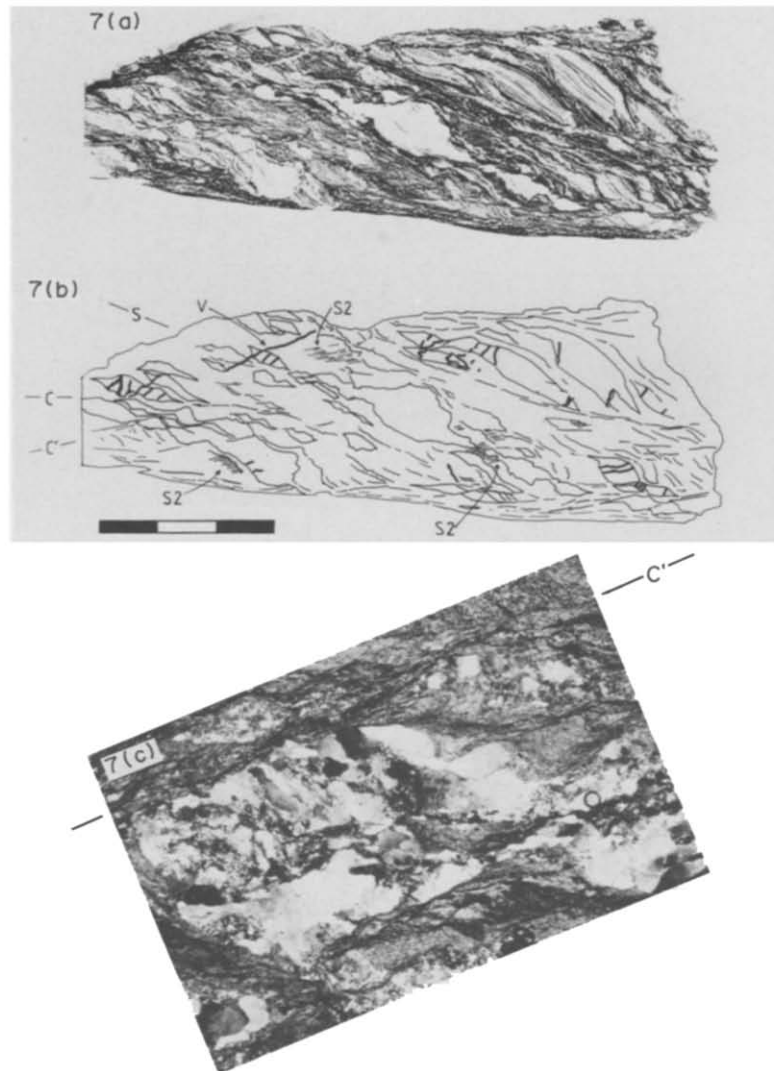


Fig. 7. Shear zone located at contact between sandstone and mélangé below Crow Hill (Fig. 2). (a) Xerographic print of large-format thin section. White lenses are vein quartz. Sample is orientated approximately vertically with west at left. (b) Drawing of same, showing *C* and *S* planes. *C'* is shear band foliation. *S*<sub>2</sub> is crenulation cleavage. *V* is narrow quartz vein at high angle to foliation. Scale bar in cm. (c) Enlargement of quartz domain from same sample, showing undulose extinction and dynamic recrystallization. Crossed polars. Scale bar 1 mm.

Fig. 8. Pressure-solution cleavage *S*<sub>2</sub>. (a) Field appearance of *S*<sub>2</sub> pressure-solution cleavage north of Humber Arm. (b) Thin section of sandstone from Summerside Formation in Corner Brook (Fig. 2) showing closely spaced pressure-solution cleavage planes (horizontal in photograph). Plane polarized light. Scale bar 1 mm.



In such areas no distinct  $F_2$  folds are seen: shortening was accommodated by tightening of earlier folds. Figure 5(d) shows a fold hinge in turbiditic limestone from the west coast of Humber Arm, southeast of Frenchman's Cove (Fig. 1). Conspicuous bed-parallel 'saddle-reef' veins contain fibrous calcite fills (Fig. 5e) that track a deformation history involving both dilation and flexural slip. They are cut by a zone of strong axial planar stylolites, interpreted to represent  $F_2$  tightening of the earlier emplacement-related folds.

### Mélange

The most distinctive feature of mélange zones within the Humber Arm Slice Assemblage is the fabric of the mélange matrix, which is characterized by anastomosing cleavage surfaces that render the matrix extremely friable. The surfaces are sometimes polished and may show slickenside striations. This fabric is equivalent to the scaly cleavage described from many cores and outcrops in accretionary terrains by Moore *et al.* (1986). In thin section (Fig. 6b), the most prominent cleavage surfaces are marked by thin opaque films. The films separate domains which are typically lenticular or lozenge shaped, within which a penetrative fabric (identical to the bed-parallel fissility of coherent terrains) is defined by preferred orientation of sheet silicates. This fabric is folded within some domains but shows abrupt changes in orientation across domain boundaries, confirming the interpretation of the latter as shear fractures. Straight and curved extension fractures are also present in the mélange matrix. These contain undeformed equant quartz (locally calcite) spar, suggesting that they were filled relatively late in the history of shearing. In thin section (Fig. 6b), the traces of most such fractures are parallel to the trace of the overall foliation, but a proportion are steeply inclined or even perpendicular to this line. Dense tangles of fractures (bottom of Fig. 6b) locally join into approximately equant patches of void-filling quartz spar. Black organic matter (similar to that described from fractures, above) occurs at the centre of some such patches. Similar sparry quartz fills irregular spaces between boudins of competent beds present as blocks in the mélange. In parts of the mélange matrix both the domain boundaries and the penetrative fabric are cut by a crenulation cleavage. The cleavage surfaces become stylolytic as they pass through or (more usually) around quartz veins. They are interpreted as post-emplacement,  $S_2$  cleavage.

In most outcrops the mélange has a grossly planar fabric, defined by the preferred orientation of scaly foliation and of inequant blocks (Fig. 10a). The orientation of this fabric may vary over distances of a few metres. In the thick mélange zone at Frenchman's Cove isolated fold hinges were measured systematically (Fig. 10b). These showed a girdle distribution oblique both to the emplacement direction deduced from fold axes in adjacent coherent slices, and to the orientation of  $F_2$  fold axial surfaces in bedded units. Unlike the folds in the slices (Waldron 1985) they do not show consistent facing

or asymmetry, indicating that blocks were rotated during mélange deformation.

### Shear zones

Most contacts between mélange and coherent slices are either discrete fault surfaces or show a progressive disruption of stratification and development of scaly foliation. In contrast, at the top of the Slice Assemblage and near its base distinct shear zones are present in which microstructures produced by plastic deformation are well developed.

At the top of the Slice Assemblage an upward transition into the metamorphic sole of the Bay of Islands Ophiolite is observed. The lowest visibly metamorphic rocks are banded chlorite schists and phyllites. Pods of psammite and metabasalt are present within the pelitic schists, suggesting that their protolith may have been similar to unmetamorphosed rocks of the Humber Arm Slice Assemblage. Sand grains are recognizable in the psammites, but in contrast to the unmetamorphosed rocks they show strong development of undulose extinction, sub-grains and local recrystallization to fine-grained polygonal quartz. In outcrop, the foliation of these schists is offset by shear fractures similar in geometry to those that produced extension of beds (shear-fracture boudinage) in unmetamorphosed units. Extension fractures filled with undeformed quartz are also present. These rocks pass upwards into mylonitic chlorite schists and then into epidote amphibolites with a strong foliation and a lineation parallel to fold axes trending due west.

At the base of the Humber Arm Slice Assemblage a shear zone is developed beneath a massive sandstone unit that caps Crow Hill in Corner Brook (Fig. 2). Figure 7 shows  $C-S$  fabrics (Berthé *et al.* 1979) in a large format thin section taken from this zone. Shear surfaces ( $C$ -planes) are marked by concentrations of fine-grained and opaque material. Large (up to 3 cm) domains of coarsely crystalline quartz are present, defining a shape fabric ( $S$ -planes), indicating transport of the upper wall of the shear zone towards the west, consistent with the regional emplacement direction, but contradicting the assertion of Brückner (1966) that this boundary represents an E-vergent thrust. The quartz domains consist of coarse quartz plates with undulose extinction and mortar structure. They are much larger than sand grains in the adjoining sediments but resemble vein quartz seen undeformed in mélange elsewhere. Siltstone domains are cut by quartz veins inclined at high angles to the  $S$ -foliation, most of which are also deformed, being folded about axial surfaces parallel to the  $S$ -planes. Some veins cut across several compositional domains, whereas other, presumably earlier veins, are cut off at domain boundaries. Within fine-grained, slaty domains, a crenulation cleavage is present, dipping slightly more steeply west than the  $C$ -planes; this is identified as the post-emplacement  $S_2$  cleavage. However, some fabric planes with this orientation cut through quartz-rich domains, offsetting and extending them in the same

sense as that inferred for the shear zone as a whole. These planes ( $C'$  in Fig. 7b) may have originated as shear bands (White *et al.* 1980) during thrusting.

#### Post-emplacment structures

In contrast to the extremely inhomogeneous, fracture-dominated and *mélange*-forming styles of deformation associated with emplacement related structures, post-emplacment deformation ( $D_2$ ) is characterized by upright to steeply inclined folds with axial planar cleavage. In the western Bay of Islands the cleavage is a sporadically developed crenulation cleavage in shales, but close to the present eastern edge of the allochthon a slaty cleavage is developed. When developed in sandstones,  $S_2$  is a pressure-solution cleavage, seen in outcrop and in thin section in Fig. 8.

## INTERPRETATION

#### Kinematics of *mélange* formation

In the Humber Arm Slice Assemblage, shear and extension fracturing are the dominant processes in the generation of *mélange*, being responsible for the formation of blocks and the development of the characteristic scaly fabric of *mélange* matrix. Two types of surface contribute to the scaly fabric: fracture surfaces form an anastomosing network, but the original bed-parallel fissility is preserved in varying orientations in domains between the fractures. Shear fractures change orientation where they pass through rock-types with contrasting anisotropy (as shown experimentally by Donath 1961). Figure 9 shows how bedding is rotated during shear-fracture boudinage as a result of curvature of the shear

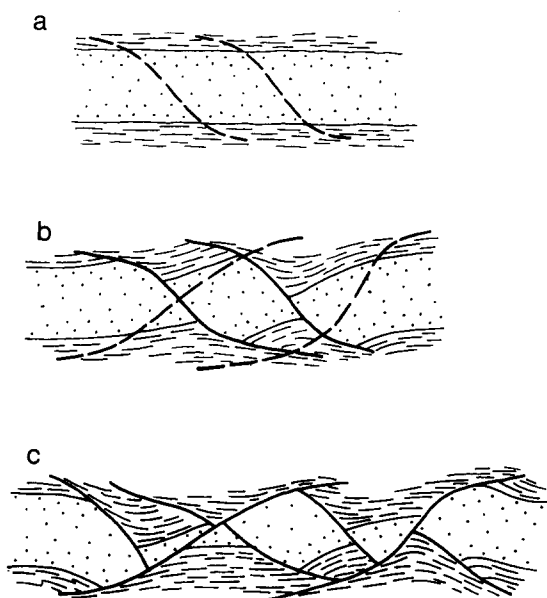


Fig. 9. Diagram to show progressive bed attenuation and development of *mélange* fabric by shear-fracture boudinage. Note rotation of bedding and bed-parallel fissility in shale (light dash ornament) resulting from slip on curved fracture surfaces (heavy lines).

surfaces. Folding within the domains was probably by flexural-slip between sheet silicate grains. Despite the abundance of microscopic brittle features, the *mélange* matrix appears ductile at mesoscopic scale. The lack of a consistent sense of asymmetry in isolated fold hinges within *mélange* indicates that the blocks containing hinges were rotated. Their present distribution (Fig. 10b) probably represents the dispersion during  $F_2$  folding of a clustered distribution produced by the *mélange*-forming event.

#### Mechanisms of deformation

Knipe (1986b) recognized four mechanisms of deformation operating in geologically young accretionary terrains: independent particulate flow, cataclastic flow, crystal plasticity and diffusion mass transfer. All four

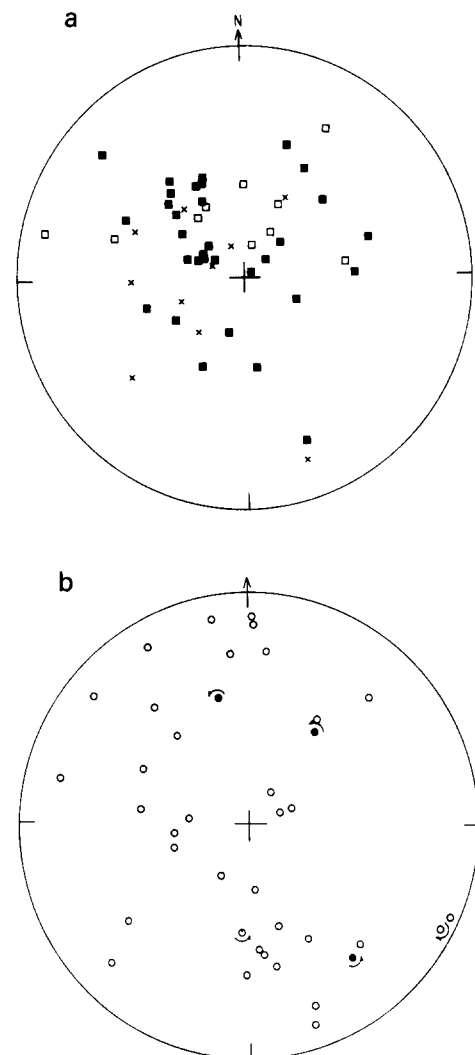


Fig. 10. Lower-hemisphere equal-area projections showing orientation of *mélange* fabric elements. (a) Fabric of *mélange* zone between slices on north coast of Humber Arm at Apsey Beach: measurements collected on 30 m traverse across continuous exposure. Open squares represent short axes of inequant blocks. Crosses are poles to bedding within inequant blocks. Filled squares represent tabular bed fragments having short axes coincident with bedding poles. (b) Orientation of isolated fold hinges in blocks from thick *mélange* zone at Frenchman's Cove. Arrows show sense of rotation indicated by fold asymmetry (open circles) or facing direction where determinable (solid circles).

processes operated during the deformational history of the Humber Arm Slice Assemblage.

Independent particulate flow was responsible for soft sediment injection structures at the base of the easterly derived flysch. Complete disaggregation during deformation is indicated by the loss of primary structures (lamination, etc.) during flow. Similar structures in a closely comparable stratigraphic setting have been described from the allochthonous Tourelle Formation in Quebec by Hiscott (1979). The injection of sand into underlying hemipelagic sediments suggests that high fluid pressures were developed at the base of the flysch, either because of a rapid increase in sedimentation rate or as a result of the onset of overthrusting of the allochthon. These injection structures are confined to this horizon, suggesting that it was less lithified than the older stratigraphic units at the time of deformation. Discrete fractures that show no evidence of grain breakage probably formed in more lithified sediments, when independent particulate flow occurred without disaggregation. Dilation is a common feature of such fracturing processes (e.g. Ashby & Verrall 1978), which would have allowed liquid hydrocarbons to penetrate between grains of the previously well compacted sediment (Figs. 3a & b). Subsequent thermal maturation produced the solid bitumen residue now observed.

Widespread veins, both in competent beds and in mélange matrix, indicate that tensile effective stresses existed, at least locally, during deformation of the slice assemblage. Two types of vein fill can be recognized. Fibrous quartz and calcite veins (Fig. 4e) represent fractures that were filled as they opened and need not have existed as continuous fluid-filled voids during deformation. Undeformed blocky and 'dog-tooth' fills formed in fractures that must have remained open during deformation. Their occurrence in a variety of orientations in weak, shaly mélange matrix (Fig. 6b) indicates that fluid pressures were close to lithostatic. High fluid pressures must have facilitated fracturing by reducing the effective normal stresses on all surfaces (Hubbert & Rubey 1959). Carson & Berglund (1986) have simulated deformation of muddy sediments and have shown that fracturing is a common response to dewatering induced by tectonic stress; if water-escape is prevented, high fluid pressures result. For tensile fractures to have formed in a variety of orientations, the normal stresses acting on all such planes must have been less than lithostatic (Fig. 11), implying a state of regional extension rather than shortening.

Cataclastic flow (i.e. flow involving breakage of grains) was probably responsible for grain size reduction in fractures in sandstone shown in Fig. 3. The fractures closely resemble those described from many geologically young accretionary terrains, both in on-land exposures (e.g. Byrne 1984) and in Deep Sea Drilling Project Cores (Lucas & Moore 1986). Cataclastic flow may also be hydraulically induced, but takes place at higher shear stresses (Lucas & Moore 1986) than independent particulate flow.

Evidence for crystal plasticity is rare in the main bulk

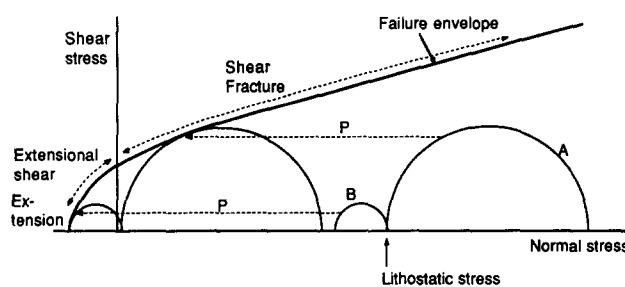


Fig. 11. Schematic Mohr diagram showing conditions for hydraulic fracturing in mélange matrix. The effect of pore pressure equal to lithostatic pressure is a translation of the Mohr circle to the left by an amount  $P$ . Under horizontal compression (minimum principal stress vertical—circle A), only shear fracturing is induced. Under a state of stress characterized by regional extension (circle B), some or most planes may suffer negative (tensile) normal stress, and failure in tension or tensile shear may occur.

of the Humber Arm Slice Assemblage, although very localized undulose extinction, sub-grain formation and even recrystallization to fine-grained polygonal quartz are seen in shear zones similar to Fig. 3(d). In contrast, shear zones near the top and bottom of the Slice Assemblage show all these features in profusion. Grain size reduction is particularly intense in the quartz domains in Fig. 7(c) where they are cut by surfaces interpreted as shear bands: this supports the interpretation of these surfaces as extensional structures associated with thrusting and not merely as products of the later crenulation cleavage.

Deformation by diffusional mass transfer is represented mainly by  $S_2$  pressure solution cleavages (Fig. 8), interpreted by Waldron (1985) to represent Acadian deformation of probable Devonian age. This deformation clearly occurred under very different conditions from the middle Ordovician emplacement event. Active accretionary terrains are characterized by low heat flow (Uyeda & Vacquier 1968); after the emplacement event the slice assemblage probably returned to a more normal geothermal gradient and Acadian deformation would therefore have occurred at higher temperature, facilitating diffusional processes. Alternatively, the Acadian deformation may have occurred at low temperature but at much lower strain rates than the emplacement event.

#### Significance of layer-parallel extension

The emplacement structures observed in the Humber Arm Slice Assemblage are strikingly similar to those described from the Franciscan and related Mesozoic–Cenozoic mélanges of the western Cordillera of North America by Moore & Wheeler (1978), Blake *et al.* (1982), Cowan (1982, 1985) and many others. These mélanges are generally regarded as products of accretion at subduction zones. Cowan (1982, 1985) points out that layer-parallel extension is characteristic of all these mélanges, and indicates a history of coaxial flattening which is difficult to reconcile with their accretionary setting. One possibility is that large-scale down-slope gravity gliding of sediments occurs (Cowan 1985, Knipe

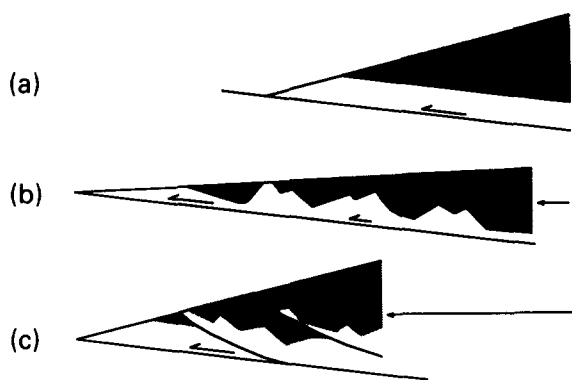


Fig. 12. Diagram to show inferred emplacement history of allochthon. In (a) allochthon has relatively steep surface slope. Tectonically induced dewatering leads to high fluid pressures beneath ophiolite 'seal', forcing a major decrease in surface slope (b), leading to coaxial layer-parallel extension in body of allochthon as its toe advances rapidly. Eventually fragmentation of the ophiolite allows escape of water. Surface slope is now below critical value for thrust movement and toe remains stationary until wedge is steepened by internal thrusting in (c).

1986a). However modern accretionary terrains do not show major slump scars or areas of tectonic denudation consistent with large-scale sliding; most seismic interpretations show only landward-dipping imbricate thrust slices (e.g. Shipley *et al.* 1982). Lucas & Moore (1986) argue that cataclastic flow in sands of the middle America Trench occurs at too shallow a depth for deformation to be explained by gravity-driven processes alone. In the Bay of Islands, extensional structures affect even the sub-ophiolite metamorphic 'aureole', suggesting that they formed at a depth at least as great as the thickness of the overlying ophiolite (10–12 km).

The overall dynamics of accretionary terrains undergoing deformation by brittle failure have been considered by Davis *et al.* (1983), Dahlen (1984) and Dahlen *et al.* (1984). They have shown that the surface slope of an accretionary wedge is a function of the coefficient of friction along the basal surface, the coefficient of internal friction controlling fracturing within the body of the wedge, the fluid pressure and whether the wedge is submarine or subaerial. Dahlen (1984) explores the effect of an increase in fluid pressure in an accretionary wedge and shows that as fluid pressure increases towards the lithostatic pressure, surface slope decreases dramatically. If the volume of the wedge and the basal décollement slope remain constant, this must result in a pronounced forward extension and thinning of the wedge by gravity spreading as shown in Fig. 12. Dahlen further shows that at extreme fluid pressures a wedge may be continuously at brittle failure in an extensional mode. Thus the development of high fluid pressures may explain the abundance of bed-parallel extensional features in the sediments of the Humber Arm Slice Assemblage, as well as the fabric of the *mélange* matrix.

Other mechanisms have been proposed that can account for extensional structures in both thrust belts and accretionary terrains. Platt & Leggett (1986) have described footwall collapse along synthetic Riedel shears

beneath thrust faults. Needham (1987) has described an analogous, ductile process of shear band development in *mélanges* in Japan. On a more regional scale, Platt (1986) has suggested that large-scale underplating of material beneath a thrust wedge may lead to extension. Any of these processes may have operated in the Humber Arm Slice Assemblage, in addition to overall control of the wedge shape by fluid pressure variation.

Figure 12 shows how the assemblage may have evolved. The overlying ophiolite (with its basal 'aureole' of metamorphic rocks) formed a seal preventing the escape of water (and oil) expelled from shales during initial deformation. As fluid pressure rose, the surface slope was lowered by gravity spreading of the allochthon. Within the body of the wedge coaxial extension would occur, disrupting the stacking order of slices and producing boudins in coherent beds. (Radial spreading may have occurred if overpressuring was localized, accounting for the formation of 'chocolate tablet' boudinage structures.) The resulting extension probably breached the impermeable seal and allowed fluids to escape, lowering the fluid pressure again. Thrusting then took over, steepening the surface slope and thickening the wedge while the toe remained stationary. The whole process was then repeated. This sequence of events may account for the presence on North Arm Mountain of internal thrusts that duplicate the ophiolite stratigraphy (Casey & Kidd 1981). When the allochthon eventually arrived over the carbonate platform sequence, the supply of water from the underlying sediments was reduced and fluid pressure fell, allowing deformation by crystal plasticity to occur at the base of the allochthon. Increased temperature due to deep burial may also have facilitated plastic deformation.

## CONCLUSIONS

Despite its occurrence in a collisional orogen, the Humber Arm Slice Assemblage shows many features found in accretionary terrains at subduction zones, and must have undergone deformation under similar conditions. The development of high fluid pressures in a brittle accretionary wedge can account for periods of coaxial bed-parallel extension and vein formation in the Humber Arm Slice Assemblage. A model involving repeated gravity spreading and shortening by thrusting can explain the mixing of blocks and tectonic slices. High fluid pressures produced by dewatering of thick or recently deposited clays and shales are primarily responsible for the development of a *mélange* terrain where a foreland fold and thrust belt would otherwise be expected.

*Acknowledgements*—This study was supported by a Senate Research grant from Saint Mary's University and by NSERC operating grant A8508 to the first author, who also acknowledges useful discussions and comments from R. K. Stevens, J. Botsford, R. N. Hiscott, R. A. Jamieson, P. Cawood, G. Stockmal and an anonymous referee.

## REFERENCES

- Ashby, M. F. & Verrall, R. A. 1978. Micromechanisms of flow and their relevance to the rheology of the upper mantle. *Phil. Trans. R. Soc. Lond.* **288A**, 59–95.
- Berthé, D., Choukroune, P. & Jégouzo, P. 1970. Orthogneiss, mylonite, and non-coaxial deformation of granites: the example of the South Armorican Shear Zone (France). *J. Struct. Geol.* **2**, 127–133.
- Blake, M. C., Jayko, A. S. & Howell, D. G. 1982. Sedimentation, metamorphism, and tectonic accretion of the Franciscan assemblage of northern California. In: *Trench Forearc Geology* (edited by Leggett, J. K.). *Spec. Publ. geol. Soc. Lond.* **10**, 433–438.
- Bosworth, W. 1984. The relative roles of boudinage and “structural slicing” in the disruption of layered rock sequences. *J. Geol.* **92**, 447–456.
- Bosworth, W. 1985. East-directed imbrication and oblique-slip faulting in the Humber Arm allochthon of western Newfoundland: Structural and tectonic significance. *Can. J. Earth Sci.* **22**, 1351–1360.
- Boyer, S. E. & Elliott, D. 1982. Thrust systems. *Bull. Am. Ass. Petrol. Geol.* **66**, 1196–1230.
- Brückner, W. D. 1966. Stratigraphy and structure of west-central Newfoundland. In: *Guidebook—Geology of Parts of Atlantic Canada* (edited by Poole, W. H.). *Geol. Ass. Can. and Min. Ass. Can. Annual Meeting, Halifax*, 137–151.
- Byrne, T. 1984. Structural geology of mélange terranes in the Ghost Rocks Formation, Kodiak Islands, Alaska. In: *Melanges, Their Nature, Origin and Significance* (edited by Raymond, L. A.). *Geol. Soc. Am. Spec. Pap.* **198**, 21–52.
- Carson, B. & Berglund, P. L. 1986. Sediment deformation and dewatering under horizontal compression: experimental results. In: *Structural Fabric in Deep Sea Drilling Project Cores from Forearcs* (edited by Moore, J. C.). *Mem. geol. Soc. Am.* **166**, 135–150.
- Casey, J. F. & Kidd, W. S. F. 1981. A parallochthonous group of sedimentary rocks unconformably overlying the Bay of Islands ophiolite complex, North Arm Mountain, Newfoundland. *Can. J. Earth. Sci.* **18**, 1035–1050.
- Cowan, D. S. 1982. Deformation of partly dewatered and consolidated Franciscan sediments near Piedras Blancas Point, California. In: *Trench Forearc Geology* (edited by Leggett, J. K.). *Spec. Publ. geol. Soc. Lond.* **10**, 439–457.
- Cowan, D. S. 1985. Structural styles in Mesozoic and Cenozoic mélanges in the western Cordillera of North America. *Bull. geol. Soc. Am.* **95**, 451–562.
- Dahlen, F. A. 1984. Noncohesive critical coulomb wedges: an exact solution. *J. geophys. Res.* **89**, 10,125–10,133.
- Dahlen, F. A., Suppe, J. & Davis, D. 1984. Mechanics of fold-and-thrust belts and accretionary wedges: cohesive Coulomb theory. *J. geophys. Res.* **89**, 10,087–10,101.
- Dahlstrom, C. D. A. 1970. Structural geology in the eastern margin of the Canadian Rocky Mountains. *Bull. Can. Petrol. Geol.* **18**, 332–406.
- Davis, D., Suppe, J. & Dahlen, F. A. 1983. Mechanics of fold-and-thrust belts and accretionary wedges. *J. geophys. Res.* **88**, 1153–1172.
- Donath, F. A. 1961. Experimental study of shear failure in anisotropic rocks. *Bull. geol. Soc. Am.* **72**, 985–990.
- Hiscott, R. N. 1979. Clastic sills and dykes associated with deep-water sandstones, Tourelle Formation, Ordovician, Québec. *J. sedim. Petrol.* **49**, 1–10.
- Hubbert, M. K. & Rubey, W. W. 1959. Role of fluid pressure in mechanics of overthrust faulting: I. Mechanics of fluid-filled porous solids and its application to overthrust faulting. *Bull. geol. Soc. Am.* **70**, 115–166.
- James, N. P. & Stevens, R. K. 1982. Anatomy and evolution of a lower Paleozoic continental margin, western Newfoundland. *11th International Congress on Sedimentology, McMaster University, Hamilton, Ontario. Field Excursion Guidebook 2B*.
- Knipe, R. J. 1986a. Microstructural evolution of vein arrays preserved in Deep Sea Drilling Project cores from Japan Trench, Leg 57. In: *Structural Fabric in Deep Sea Drilling Project Cores from Forearcs* (edited by Moore, J. C.). *Mem. geol. Soc. Am.* **166**, 75–87.
- Knipe, R. J. 1986b. Deformation mechanism path diagrams for sediments undergoing lithification. In: *Structural Fabric in Deep Sea Drilling Project Cores from Forearcs* (edited by Moore, J. C.). *Mem. geol. Soc. Am.* **166**, 151–160.
- Lucas, S. E. & Moore, J. C. 1986. Cataclastic deformation in accretionary wedges. Deep Sea Drilling Project Leg 66, southern Mexico, and on-land examples from Barbados and Kodiak Islands. In: *Structural Fabric in Deep Sea Drilling Project Cores from Forearcs* (edited by Moore, J. C.). *Mem. geol. Soc. Am.* **166**, 89–103.
- Malpas, J. & Stevens, R. K. 1977. The origin and emplacement of the ophiolite suit with examples from western Newfoundland. *Geotectonics* **11**, 453–466.
- McCaig, A. M. 1983. P–T conditions during emplacement of the Bay of Islands ophiolite complex. *Earth planet. Sci. Lett.* **63**, 459–473.
- Moore, J. C. & Wheeler, R. L. 1978. Structural fabric of a mélange, Kodiak Islands, Alaska. *Am. J. Sci.* **278**, 739–765.
- Moore, J. C., Roeske, S., Lundberg, N., Schoonmaker, J., Cowan, D. S., Gonzales, E. & Lucas, S. E. 1986. Scaly fabrics from Deep Sea Drilling Project cores from forearcs. In: *Structural Fabric in Deep Sea Drilling Project Cores from Forearcs* (edited by Moore, J. C.). *Mem. geol. Soc. Am.* **166**, 55–68.
- Needham, T. 1987. Asymmetric extensional structures and their implications for the generation of mélanges. *Geol. Mag.* **124**, 311–318.
- Platt, J. P. 1986. Dynamics of orogenic wedges and the uplift of high-pressure metamorphic rocks. *Bull. geol. Soc. Am.* **97**, 1037–1053.
- Platt, J. P. & Leggett, J. K. 1986. Stratal extension in thrust footwalls, Makran accretionary prism: implications for thrust tectonics. *Bull. Am. Ass. Petrol. Geol.* **70**, 191–203.
- Shiple, T. H., Ladd, J. W., Buffler, R. T. & Watkins, J. S. 1982. Tectonic processes along the Middle American Trench inner slope. In: *Trench Forearc Geology* (edited by Leggett, J. K.). *Spec. Publ. geol. Soc. Lond.* **10**, 95–106.
- Stevens, R. K. 1965. Geology of Humber Arm, West Newfoundland. Unpublished M.Sc. thesis, Memorial University, Newfoundland.
- Stevens, R. K. 1970. Cambro-Ordovician flysch sedimentation and tectonics in West Newfoundland and their possible bearing on a Proto-Atlantic Ocean. In: *Flysch Sedimentology in North America* (edited by Lajoie, J.). *Geol. Ass. Can. Spec. Pap.* **7**, 165–177.
- Uyeda, S. & Vacquier, V. 1968. Geothermal and geomagnetic data in and around the island arc of Japan. In: *The Crust and Upper Mantle of the Pacific Area* (edited by Knopoff, L.). *Am. Geophys. Union Geophys. Monograph* **12**, 349–366.
- White, S. H., Burrows, S. E., Carreras, J., Shaw, N. D. & Humphreys, F. J. 1980. On mylonites in ductile shear zones. *J. Struct. Geol.* **2**, 175–187.
- Williams, H. 1985. Steenville Map Area, Newfoundland. *Geol. Surv. Can. Map* **1579A**.
- Williams, H. & Cawood, P. 1986. Relationships along the eastern margin of the Humber Arm Allochthon between Georges Lake and Corner Brook, western Newfoundland. Current Research Part A. *Geol. Surv. Can. Pap.* **86-1A**, 759–765.